COMPUTER METHODS IN MATERIALS SCIENCE

2023, vol. 23, no. 4, 19–29
https://doi.org/10.7494/cmms.2023.4.0817

Simulation analysis for the efficiency enhancement of Sb_2S_3 solar cell using SCAPS-1D

Mubarak Hamad Oglah*, Watban Ibrahim Mahmood, Nawras Basheer Adday

Department of Mechanics Engineering, College of Al-Shirgat Engineering, Tikrit University, Iraq.

Abstract

The simulation analysis was performed to enhance the efficiency of Sb_2S_3 solar cells using the SCAPS-1D software. The Sb_2S_3 compound was used as the absorber layer in the solar cell. The simulation was conducted to verify the efficiency and accuracy of the results obtained from the program. The results were found to be in agreement with the practical results. The original cell's efficiency was 11.47% with a fill factor of 61.18%, and after the simulation, the efficiency was found to be 11.43% with a fill factor of 61.2%.

To enhance the efficiency of the solar cell, a reflective background layer (BSL) was added. Different BSL layers were examined, including SnS, Si, CIGS, CZTSSe, and CU_SbS_3, and the best reflective layer was found to be $CUSbS_3$. The solar cell structure was designed as follows: glass/Mo/$CUSbS_3$/Sb_2S_3/CdS/i:ZnO/AL:ZnO. After adding the reflective layer, the efficiency of the solar cell was found to be 20.59% with a fill factor of 87.53%.

The results suggest that adding reflective layers to solar cells can enhance their performance and increase their efficiency.

Keywords: numerical simulation, efficiency, solar cells, Sb_2S_3 compound, SCAPS-1D

1. Introduction

The use of sustainable and renewable energy sources such as solar energy has become increasingly important in recent years due to the negative environmental impact of conventional fuels. While silicon solar cells have been the standard for many years, inorganic layered solar cells, such as those based on antimony sulfide (Sb_2S_3), have gained attention due to their lower cost and high stability, as mentioned in the paper by Lee Y.-J. et al. (2014). Researchers have carried out numerous studies on Sb_2S_3 for the purpose of improving the conversion efficiency of solar cells. One approach is to modify the middle layer by adding background absorbent layers (BSL) to the cell to recover the wasted energy and direct it towards the cell to convert it into additional energy by Louwen et al. (2016).

Various studies have been conducted by researchers to enhance the conversion efficiency of solar cells based on the compound Sb_2S_3. Some of these studies have focused on the integration of different materials and layers to improve the performance characteristics of Sb_2S_3-based solar cells by (Green et al., 2016; Gupta et al., 2011; Mukherjee, 2020; Mukherjee et al. 2014). One study investigated the impact of incorporating a ZnS interlayer on Sb_2S_3-based solar cells to enhance their

*Corresponding author: mubarak@tu.edu.iq
ORCID ID's: 0000-0002-4368-5594 (M.H. Oglah), 0009-0002-0105-1259 (W.I. Mahmood), 0009-0004-7851-2978 (N.B. Adday)

conversion efficiency by Zeng et al. (2016). The research revealed that the addition of the ZnS interlayer significantly improved the solar cells' energy conversion efficiency. The specific efficiency improvement achieved was noted to be 5.01% in the context of this study.

Another study focused on enhancing the performance of a CdS/Sb_2S_3 hybrid junction solar cell by introducing an insulating layer of magnesium-doped tin oxide (SnO). The insulating layer was strategically applied to optimize the solar cell's efficiency. The objective of this research was to achieve high-efficiency solar cells by utilizing an innovative insulating layer on top of the CdS/Sb_2S_3 hybrid junction by Zhang F. et al. (2020).

Both studies underline the ongoing efforts to enhance the efficiency of solar cells based on Sb_2S_3 by incorporating novel materials, interlayers, and treatments. These approaches aim to overcome challenges and limitations while maximizing the potential for energy conversion. Researchers are exploring various techniques to optimize the performance of Sb_2S_3-based solar cells, which could contribute to the advancement of solar energy technology, as noted by Choi et al. (2014a).

In a study conducted by Ma (2020), a thin film doped with Ti:Sb_2S_3 was prepared using a simple spin method. The addition of Ti:Sb_2S_3 to the solar cell led to a significant increase in conversion efficiency, specifically by 41% compared to cells containing the original Sb_2S_3. The study examined the impact of different concentrations of Ti impurities on cell performance. It was observed that increasing the concentration of Ti doping up to a certain level (6%) improved cell efficiency, with the highest efficiency ratio achieved being 2.70%. The improved performance of Ti:Sb_2S_3-based devices was attributed to enhanced optical absorption properties of the doped thin film by Faheem et al. (2019).

Another study, conducted by Chen J. et al. (2021), introduced graphene/polymer composite chips as the gap transport layer in Sb_2S_3/TiO_2-BnpHJ (Bulk Nanoporous Heterojunction) solar cells. This study was the first to utilize this composite material for the gap transport layer. The Sb_2S_3/TiO_2-BnpHJ solar cells incorporating the graphene/polymer composite achieved a conversion efficiency of 5.72% along with good stability.

Many compounds have been studied for their potential application in photovoltaic devices. SnS by Nair (2016), is a semiconductor material with a layered crystal structure. It was investigated for its ability to absorb sunlight and convert it into electricity in thin-film solar cells. Cu_2O by Lee Y.S. et al. (2014), is a p-type semiconductor with a direct bandgap. It has been explored for its potential use in solar cells and photodetectors. Cu_2SnS_3 by Berg et al. (2012), is a compound semiconductor with a suitable bandgap for solar energy absorption. It has been studied as an absorber material in thin-film solar cells. Cu_2GeS_3 by Jin et al. (2017), is another compound semiconductor with tunable properties. It has been considered for its potential application in photovoltaic devices by Xue et al (2017), GeSe is a layered semiconductor material. It has been investigated for its potential use in photovoltaics and other optoelectronic applications. Sb_2S_3 by Moon et al. (2010), as mentioned previously, is a compound semiconductor with promising characteristics for solar cells, including suitable energy levels and absorption properties. Sb_2Se_3 by Liu et al. (2017), is a related compound to Sb_2S_3 and has been explored for its potential use in solar cell applications. All of these compounds have unique properties that make them interesting candidates for solar cell materials.

These studies emphasize the potential of doping Sb_2S_3 with different materials and utilizing innovative composite structures to enhance the efficiency and stability of solar cells. The introduction of novel materials, like Ti:Sb_2S_3 and graphene/polymer composites, demonstrates the ongoing exploration of advanced techniques to optimize various aspects of solar cell performance, including absorption, charge transport, and stability by Chen Z. & Chen G. (2020). These efforts contribute to the advancement of photovoltaic technology and the potential for more efficient and sustainable energy conversion.

The proposed study aims to use SCAPS-1D software to simulate the performance of a (glass/Mo/Sb_2S_3/CdS/i:ZnO/AL:ZnO) solar cell and evaluate its performance after adding an interfacial absorbent layer (SnS, Si, CIGS, CZTSSe, $CUSbS_3$) to choose the best.

The simulation results from SCAPS-1D will help determine the effect of the different interfacial absorbent layers on the performance characteristics of the solar cell. This study could contribute to the development of more efficient and cost-effective solar cells, which could play a vital role in meeting the increasing demand for sustainable energy sources.

2. Structure of the solar cell

As shown in Figure 1 (by Eisele et al., 2003; Michaelson, 1977), the solar cell under investigation is composed of:

- window layer (glass/Mo/Sb_2S_3/CdS/i:ZnO/AL:ZnO):
  - glass: the substrate upon which the solar cell is built;
  - Mo (molybdenum): a back contact layer that provides electrical connection and support to the rest of the cell;

- Sb_2S_3 (antimony sulfide): a light-absorbing layer that absorbs photons and generates electron-hole pairs;
- CdS (cadmium sulfide): a buffer layer that enhances the absorption of optical photons and improves the cell's efficiency;
- i:ZnO (intrinsic zinc oxide): a transparent conducting oxide layer that helps with electron transport;
- AL:ZnO (aluminum-doped zinc oxide): a transparent conducting layer that allows light to pass through and helps in electron collection;

– buffer layer (CdS) (CdS is the second layer, functioning as a buffer between the window layer and the absorbing layer; it helps optimize the cell's performance by enhancing photon absorption and facilitating electron-hole separation);

– absorbing layer (Sb_2S_3) (Sb_2S_3 is the primary layer responsible for absorbing photons and creating electron-hole pairs; it has a high absorption coefficient and p-type conductivity, which means it generates positive charge carriers – holes – upon light absorption);

– contacts:
- front ohmic contact (this is typically a transparent conductive layer that helps collect the electrons generated in the absorbing layer; it ensures efficient electron extraction);
- back Schottky contact (the Schottky contact on the back – Mo metal in our description – serves as a barrier that allows electrons to flow in one direction, assisting in collecting the generated current).

The described solar cell structure follows a specific design to optimize light absorption, charge separation, and electron transport, ultimately leading to the efficient conversion of sunlight into electricity.

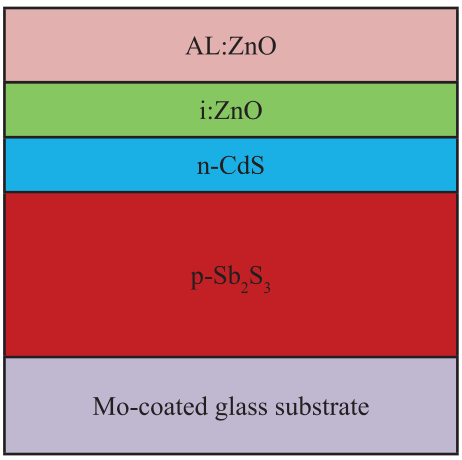

Fig. 1. The schematic structure of Sb_2S_3 cell

3. Description of solar cell performance

There are some parameters that collectively describe the efficiency and overall performance of a solar cell:

– short circuit current density (J_{sc}):
- the maximum current density that a solar cell can produce when its terminals are short-circuited (i.e., no external load connected); represents the current generated by the solar cell in the presence of maximum sunlight;
- a critical parameter as it indicates the cell's ability to generate current under optimal illumination conditions;

– open circuit voltage (V_{oc}):
- the voltage across the terminals of the solar cell when there is no external load attached (i.e., open circuit condition); represents the maximum voltage the cell can produce;
- a measure of the cell's ability to separate and maintain charges (electron-hole pairs) in the absence of a current flow;

– maximum power (P_{max}):
- the maximum power output that the solar cell can deliver to an external load; occurs at a specific voltage and current point on the current–voltage (*I-V*) characteristic curve;
- this point represents the optimal operating condition where the cell generates the most power;

– fill factor (*FF*):
- a measure of how effectively the cell's maximum power is used; the ratio of the actual maximum power output to the product of V_{oc} and J_{sc}; mathematically, $FF = (P_{max}) / (V_{oc} \cdot J_{sc})$;
- a higher fill factor indicates better utilization of the cell's potential power.

The characteristic curve (*I-V* curve) you mentioned is a graphical representation of the relationship between the current (*I*) and voltage (*V*) across the terminals of the solar cell under varying external load conditions. By analyzing this curve, we can determine the aforementioned performance parameters:

– J_{sc} is obtained from the current axis at zero voltage (short-circuit condition);

– V_{oc} is obtained from the voltage axis at zero current (open-circuit condition);

– P_{max} is the highest point on the curve, where the product of current and voltage is maximized;

– *FF* is calculated as described above, using the ratio of P_{max}, V_{oc}, and J_{sc}.

These parameters collectively describe the efficiency and overall performance of a solar cell. Engineers and researchers analyze them to understand how effectively a solar cell converts sunlight into electricity and to optimize its design and operation

The maximum current can be obtained from the following equation:

$$J(V) = J_{sc} - J_{dark}(V) \tag{1}$$

where J_{dark} is the dark stream intensity:

$$J_{dark}(V) = J_0\left(e^{\frac{qV}{K_BT}} - 1\right) \tag{2}$$

By substituting Equation (2) in the ideal diode equation, the equation is:

$$J(V) = J_{sc} - J_0\left(e^{\frac{qV}{K_BT}} - 1\right) \tag{3}$$

In the same way, we have:

$$J_{sc}(V) = J(V) + J_0\left(e^{\frac{qV}{K_BT}} - 1\right) \tag{4}$$

where V is the potential during the junction, J_0 is the saturation current during the night, T is the temperature [K].

An open circuit voltage V_{oc} is formed when the terminals of the solar cell are not connected to each other. It is the maximum effort that solar cells can provide. The optical current density J_{ph} of a simple $P - n$ junction directly affects V_{oc} as it is given in the following equations by Koltsov et al. (2023):

$$V_{oc} = \frac{K_BT}{q}\ln\left(\frac{J_{ph}}{J_o} + 1\right) \tag{5}$$

The ratio between the maximum power $P_{max} = J_{mp} \times V_{mp}$ generated by the solar cells and the output J_{sc}, V_{oc} is the filling factor FF.

$$FF = \frac{J_{mp} \times V_{mp}}{V_{oc}J_{sc}} = \frac{P_{\max}}{V_{oc}J_{sc}} \tag{6}$$

The current density and the maximum voltage that the solar cell can generate are J_{mp}, V_{mp}.

The conversion efficiency η represents the ratio between the maximum power generated by the solar cells and the power falling on them, as in the following equation:

$$\eta = \frac{P_{\max}}{P_{in}} = \frac{J_{sc}V_{oc}FFJ}{P_{in}} \tag{7}$$

The P_{in} radiation value is 1000 w/m^2 of the spectrum under an optical air mass 1.5 AM and is considered a standard in solar cells to measure the conversion efficiency. It is a measure of the incident power as a function of the area of the solar cell by Jaramillo-Quintero et al. (2021).

4. Absorbent materials

The choice of semiconductor materials is crucial for the efficiency and performance of solar cells. Factors such as the energy gap, recombination speed, carrier lifetime, and absorption coefficient play a significant role in determining the suitability of materials for solar energy conversion.

Researchers are currently working on developing new materials and compounds to enhance solar cell performance, as noted by Li et al. (2022). Some of these materials include Perovskite Solar Cells (Lewis, 2016; Snaith, 2018; Zhang W. et al., 2016; Zhou et al., 2014), Organic Solar Cells (Choi et al., 2014a), Tandem Solar Cells (Green et al., 2014), Quantum Dots (Polman et al., 2016), 2D Materials (Xiao et al., 2020).

The goal is to find materials that can effectively absorb a wide range of solar radiation while being cost-effective and environmentally friendly. As research continues, these new materials hold the potential to revolutionize the efficiency and accessibility of solar energy technology.

5. Optical properties of Sb_2S_3

Sb_2S_3 (antimony trisulfide) is a semiconductor material that has gained interest in photovoltaic applications due to its favorable optical properties for solar energy conversion. Sb_2S_3 has a relatively high absorption coefficient, which means it can efficiently absorb a significant portion of incident sunlight. This property is essential for converting light energy into electron-hole pairs within the material. Sb_2S_3 has a moderate band gap of approximately 1.65 eV. This band gap allows it to absorb photons in the visible and near-infrared regions of the electromagnetic spectrum. The ability to absorb light in these energy ranges is crucial for solar cells to capture a substantial portion of solar radiation. The color of Sb_2S_3 is typically dark brown or black, indicating its ability to absorb visible light. However, its transparency can be improved by engineering thin films or nanostructures, making it suitable for applications where semitransparent or colored solar cells are desired. Sb_2S_3 is a direct band gap semiconductor, which means that electron transitions that contribute to absorption and emission of light occur without a change in the electron's momentum. This property enhances the efficiency of light absorption and emission processes. Sb_2S_3 can effectively generate electron-hole pairs (excitons) when exposed to light. This is a fundamental requirement for photovoltaic materials, as these excitons can be separated and contribute to the flow of electric current in a solar cell. The optical properties of Sb_2S_3 can be tuned by controlling its particle size and structure. This allows researchers to optimize its performance for specific applications, such as thin-film solar cells or quantum dot sensitized solar cells.

Due to its band gap and absorption properties, Sb_2S_3 can be used in tandem solar cell configurations where multiple layers of different materials are stacked to capture a broader spectrum of sunlight. This can lead to higher overall efficiency in solar energy conversion.

While Sb_2S_3 exhibits promising optical properties for solar energy applications, it is worth noting that its practical use in solar cells also depends on other factors, such as its electrical properties, stability, and the ability to fabricate high-quality films by Kondrotas et al., 2018 (as in Figure 2).

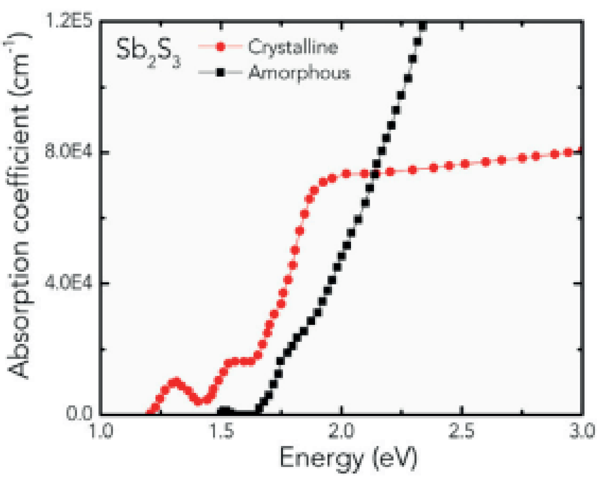

Fig. 2. Electronic and optical properties of Sb_2S_3

6. Discussion of the results

The work was divided into two parts:
- **Part I – simulation using SCAPS-1D:** in this part, we conducted simulations of the Sb_2S_3 solar cell using the SCAPS-1D program. The purpose of this simulation was to validate the accuracy of the model and its predictions by comparing the simulation results with the known characteristics of the original Sb_2S_3 solar cell.
- **Part II – addition of reflection layers:** the second part involved enhancing the solar cell's output by adding reflection layers beneath the absorption layer. Reflection layers are designed to improve light trapping and absorption within the solar cell. By introducing specific materials as layers beneath the absorption layer, we aimed to optimize the cell's performance in terms of light absorption and conversion efficiency.

The purpose of adding reflection layers is to improve light trapping, minimization of photon loss and enhanced absorption.

6.1. Part I. Simulate the origin cell

Solar cell structure

The original solar cell consists of several layers arranged in the following sequence:
- glass/Mo/Sb_2S_3/CdS/i:ZnO/Al:ZnO;
- glass base: the substrate upon which the solar cell is built;
- Mo (molybdenum): back contact layer for electrical connection;
- Sb_2S_3 (antimony trisulfide): primary absorbing layer with an energy gap of 1.65 eV and a certain thickness;
- CdS (cadmium sulfide): matching layer with an energy gap of 2.4 eV and a thickness of 0.05 μm. i:ZnO (intrinsic zinc oxide); transparent conducting oxide layer for electron transport;
- Al:ZnO (aluminum-doped zinc oxide): transparent conducting layer with an energy gap of 3.3 eV.

Simulation and comparison

After conducting a simulation of the solar cell, the results were found to be identical to the original cell's behavior. This is a significant validation of the simulation model's accuracy. Table 1 presents a comparison between the output parameters (current-voltage characteristics, efficiency) of the original cell and the simulated cell. Figure 3 depicts the energy levels within the original solar cell.

Table 1. Comparing the output of the cell after the simulation with the original cell

No.	Cell	V_{oc} [V]	J_{sc} [mA/cm^2]	*FF* [%]	η [%]
1	original cell Sb_2S_3	0.967	19.18	61.82	11.47
2	cell after simulation	0.996	18.74	61.20	11.43

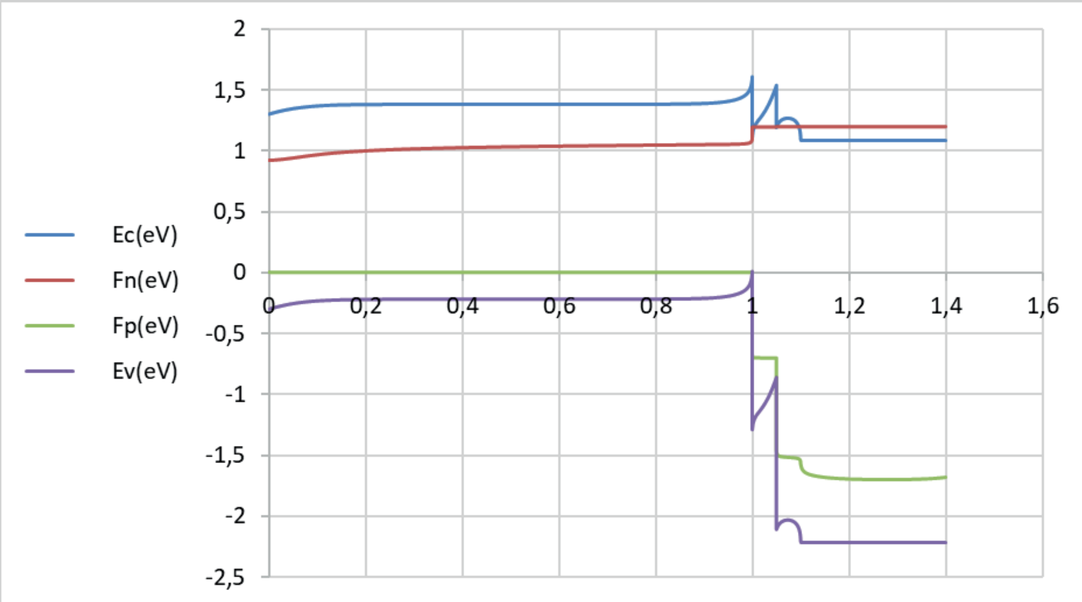

Fig. 3. Energy levels of the original solar cell

6.2. Part II. Adding an interfacial absorbent layer

In Part II of work, we focused on enhancing the solar cell's performance by adding an interfacial absorbent layer beneath the absorption layer (Sb_2S_3).

Materials used as reflection layers are SnS, Si, CIGS (copper indium gallium selenide), CZTSSe (copper zinc tin sulfide selenide), and $CUSbS_3$ (copper antimony sulfide). Among these, $CUSbS_3$ with a thickness of 0.05 µm and an energy gap of 1.5 eV was found to be the most effective reflection layer.

Adding the $CUSbS_3$ reflection layer led to significant improvements in the solar cell's performance. The open circuit voltage (V_{oc}) increased from V0.996 to V1.06, and the short circuit current density (J_{sc}) increased from 18.74 mA/cm^2 to 22.11 mA/cm^2.

As in Table 2, the conversion efficiency (η) of the solar cell increased from 11.43% for the original cell to 20.59% after incorporating the best reflection layer ($CUSbS_3$). This indicates a substantial improvement in the ability of the cell to convert sunlight into electricity.

The voltage–current (*I-V*) characteristics curve of the solar cell was visibly affected by the addition of the reflection layer. This is due to the enhanced light absorption resulting from reflection off the reflection layer, leading to increased incident light on the absorption layer, see Figure 4.

Table 3 shows material parameters used as reflection layers in the cell, the reflection layer helped improve conversion efficiency by reflecting back photons that are not initially absorbed by the absorption layer. This increases the concentration of charge carriers and reduces recombination, contributing to higher photocurrent. The enhanced reflection also leads to improved Ohmic conductivity and better contact.

$CUSbS_3$ was determined to be the best reflection layer, leading to the highest increase in conversion efficiency. This could be attributed to factors such as its energy gap, electronic affinity, and work function, which contribute to improved conductivity and efficient light absorption.

Overall, the results demonstrate that the addition of an interfacial absorbent layer (reflection layer) can significantly enhance the performance of the Sb_2S_3 solar cell, leading to increased conversion efficiency, improved open circuit voltage, and higher short circuit current density. The specific properties of $CUSbS_3$ make it a favorable choice for this purpose.

Quantum efficiency measures the ratio of carriers (electron-hole pairs) collected in the solar cell to the number of photons that fall on the cell. It provides insights into how effectively the solar cell converts incoming photons into electron-hole pairs.

By adding the $CuSbS_3$ reflection layer to the solar cell, we observed a change in the quantum efficiency as a function of the wavelength of light. The quantum efficiency curve, as depicted in Figure 5, showed variations corresponding to the change in reflection layers. The quantum efficiency exhibited a notable increase, reaching its highest value around a wavelength of approximately 380 nm. This peak represents the wavelength at which the solar cell is most efficient in converting light into electron-hole pairs. This efficiency increase is attributed to the maximum absorption of photons that have undergone reflection from the reflection layer.

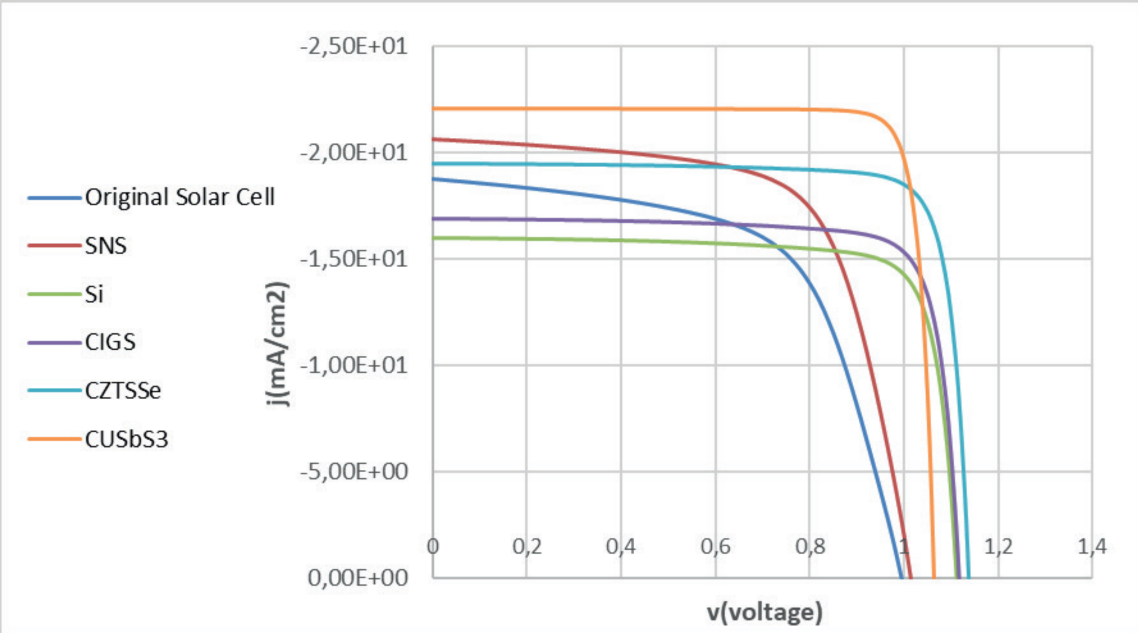

Fig. 4. The *I-V* curve of the cell before and after adding the reflection layers

Table 2. The output of the original cell compared to the cell after adding the reflection layers

Material	J_{sc} [mA/Cm^2]	V_{oc} [V]	*FF* [%]	η [%]
Original cell	18.74	0.996	61.20	11.43
SnS	20.60	1.010	66.68	13.94
Si	16.00	1.110	80.77	14.37
CIGS	16.92	1.110	81.41	15.39
CZTSSe	19.50	1.130	83.68	18.53
$CuSbS_3$	22.11	1.060	87.53	20.59

Table 3. Parameters of the used reflection layers

Parameters	Symbol [unit]	SnS (Omrani, 2018)	Si (Boumaour, 2019)	CIGS (Dixit, 2023)	CZTSSe (Abdelbaki & Labbani, 2017)	$CuSbS_3$ (Olopade, 2017)
Thickness	*W* [μm]	0.1	0.1	0.05	0.05	0.05
Bandgap	*Eg* [eV]	1.1	1.12	1.05	1.30	1.50
Electron affinity	χ [eV]	4.2	4.05	4.14	4.10	4.20
Dielectric permittivity	ϵr	12.5	11.9	10.00	113.60	10.00
CB effective density of states	N_C [cm^{-3}]	1.000e + 19	2.580e + 19	1.000e + 18	2.220e + 18	2.200e + 18
VB effective density of states	N_V [cm^{-3}]	4.130e + 19	2.650e + 19	1.000e + 18	1.800e + 19	1.800e + 19
Electron thermal velocity	V_n [cm/s]	1.000e + 7	1.000e + 7	1.000e + 7	1.000e + 7	1.000e + 7
Hole thermal velocity	V_p [cm/s]	1.000e + 7	1.000e + 7	1.000e + 7	1.000e + 7	1.000e + 7
Electron mobility	μ_n [cm^2/v·s]	2.500e + 1	1.350e + 3	3.00e + 1	1.000e + 2	1.000e + 2
Hole mobility	μ_p [cm^2/v·s]	1.000e + 2	4.500e + 2	1.500e + 1	2.500e + 1	2.500e + 1
Shallow uniform donor density	ND [1/cm^3]	0	0	0	0	0
Shallow uniform acceptor density	NA [1/cm^3]	1.000e + 18	1.000e + 17	1.000e + 19	1.000e + 19	1.000e + 20
Coefficient absorption	α [1/cm]	–	–	–	–	–

The quantum efficiency curve approaching a square-like shape at the peak (380 nm) indicates an ideal condition for the solar cell's operation. This is because the solar cell is absorbing photons efficiently and generating a significant number of electron-hole pairs, leading to higher overall efficiency.

As the wavelength increases beyond approximately 380 nm, the quantum efficiency starts to decrease. This decrease is due to factors such as a lower diffusion length and minimal absorption of light at longer wavelengths. These factors limit the ability of the solar cell to generate electron-hole pairs efficiently.

The addition of the reflection layer, specifically Cu_SbS_3, has a significant impact on the quantum efficiency curve. It enhances the efficiency of photon absorption and electron-hole pair generation, resulting in an overall improvement in the quantum efficiency of the solar cell.

This analysis underscores how the choice of reflection layers can not only influence the electrical characteristics of the solar cell, as discussed previously, but also its optical properties and the efficiency with which it converts light into usable electrical energy by optimizing the reflection layers and other aspects of the solar cell's structure.

To represent the relationship between quantum efficiency (Q_E) and wavelength (λ) in terms of the absorption coefficient (R_λ) from the upper surface of the solar cell.

We use the equation given by Rau et al. (2001):

$$Q_E = 1.24 \frac{R_\lambda}{\lambda} \tag{8}$$

where: Q_E is the quantum efficiency, R_λ is the absorption coefficient from the upper surface of the solar cell, λ is the wavelength of the incident light.

This equation describes the inverse proportionality between the quantum efficiency (Q_E) of the solar cell and the wavelength (λ) of the incident light. Quantum efficiency refers to the ratio of the number of charge carriers (electron-hole pairs) generated in the solar cell to the number of photons incident on the cell. In other words, it quantifies how efficiently the solar cell converts photons into usable electrical current.

The absorption coefficient (R_λ) reflects the ability of the solar cell material to absorb light at a specific wavelength. It indicates how strongly light of a particular wavelength is absorbed as it passes through the material. A higher absorption coefficient implies stronger absorption of light and, consequently, a higher likelihood of generating electron-hole pairs.

The equation indicates that quantum efficiency (Q_E) increases with increasing absorption coefficient (R_λ) and decreasing wavelength (λ). This relationship makes sense: when the absorption of light is higher, more electron-hole pairs are generated, resulting in a higher quantum efficiency. Additionally, shorter wavelengths are more energetic and are generally absorbed more effectively.

The constant factor 1.24 in the equation is a conversion factor that relates wavelength to energy in electronvolts (eV). It allows for expressing the quantum efficiency in terms of energy-related quantities.

This relationship helps explain the behavior observed, where quantum efficiency decreases as wavelength increases due to the decreasing absorption at longer wavelengths. It also highlights the importance of optimizing material properties and layer configurations in solar cells to maximize quantum efficiency and overall energy conversion efficiency.

In Figure 5, the energy levels of the original solar cell structure are presented. The absence of a voltage barrier or a negative value in relation to electrons at the back surface. This indicates an accumulation of electrons at the back surface, which can potentially lead to an increased likelihood of recombination. Recombination refers to the process where electron-hole pairs recombine and neutralize each other, reducing the efficiency of the solar cell.

In Figure 6, the energy levels of the solar cell are shown after adding the best reflection layer ($CUSbS_3$). The modified cell structure now includes additional layers, and the arrangement becomes glass/Mo/$CUSbS_3$/Sb_2S_3/CdS/i:ZnO/Al:ZnO.

The addition of the $CUSbS_3$ reflection layer has notable effects on the energy levels. Where the modified structure results in the generation of a high-voltage barrier for electrons. This barrier prevents excessive accumulation of electrons at the back surface, reducing the chances of recombination. This is important for maintaining efficient charge carrier separation. Conversely, there is a low voltage barrier for holes (positive charge carriers). This configuration allows a larger number of carriers, including holes, to reflect back towards the absorption layer (Sb_2S_3).

The net effect of these changes is an increase in the open circuit voltage (V_{oc}) and the short circuit current density (J_{sc}) of the solar cell. The increase in V_{oc} and J_{sc} ultimately contributes to an improvement in the conversion efficiency (η) of the solar cell. This aligns with your observations that the modified cell with the reflection layer exhibited higher efficiency.

By engineering the energy levels and charge carrier dynamics within the solar cell structure, its performance can be enhanced, recombination losses reduced, and the conversion of sunlight into electricity optimized.

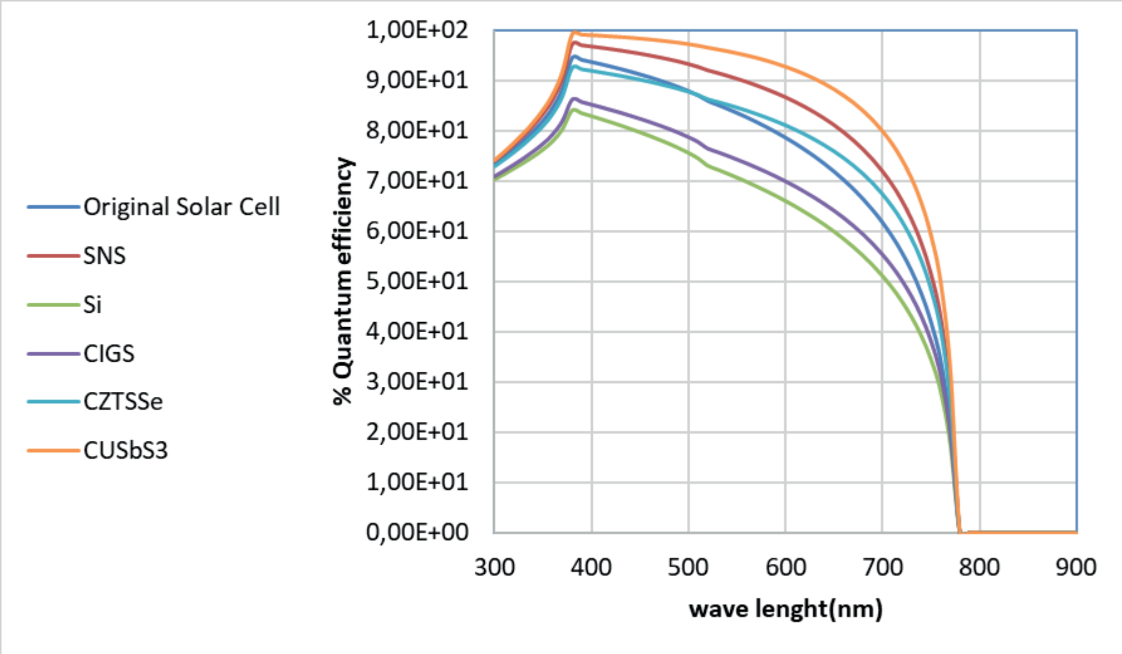

Fig. 5. Quantum efficiency values of the solar cell before and after adding the reflection layer

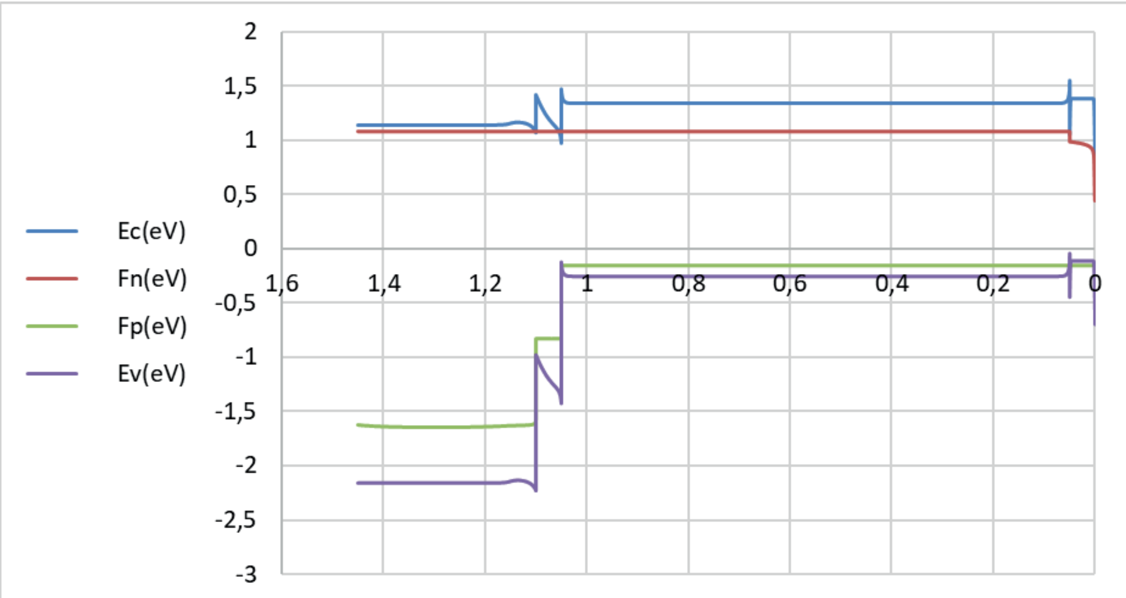

Fig. 6. Energy levels of the best reflection layer $CuSbS_3$

These findings emphasize the significance of understanding and controlling the energy levels and charge transport mechanisms within the solar cell to achieve higher efficiency and improved overall performance.

7. Conclusions

The study aimed to enhance the photovoltaic cell based on Sb_2S_3 through improvements and changes to its structure. The simulation of the original solar cell structure using the SCAPS-1D program yielded results that were consistent with or very close to practical results. This indicates the reliability and accuracy of the simulation tool in predicting real-world behavior, offering a cost-effective and time-efficient approach to analysis. Different adaptive layers were considered, and it was concluded that CdS is the most effective among them, demonstrating the significance of maintaining certain layers for optimal performance. Furthermore, the addition of back reflection layers (BSL) also improved the cell's efficiency. Of the materials considered, $CUSbS_3$

was identified as the best reflection layer. The integration of $CUSbS_3$ as a reflection layer led to a substantial increase in the conversion efficiency (η), resulting in a notable enhancement of the overall performance of the solar cell. These conclusions highlight the effectiveness of our approach in improving the Sb_2S_3-based solar cell's performance through systematic changes and enhancements to its structure. The consistent simulation results and the quantifiable increase in efficiency underscore the importance of thoughtful material selection and design optimization in achieving higher energy conversion efficiency in solar cells.

Referances

Abdelbaki, Ch., & Labbani, R. (2017). Study of CZTS and CZTSSe solar cells for buffer layers selection. *Applied Surface Science*, *424*(2), 251–255. https://doi.org/10.1016/j.apsusc.2017.05.027.

Berg, D.M., Djemour, R., Gütay, L., Zoppi, G., Siebentritt, S., & Dale, P.J. (2012). Thin film solar cells based on the ternary compound Cu_2SnS_3. *Thin Solid Films*, *520*(19), 6291–6294. https://doi.org/10.1016/J.TSF.2012.05.085.

Boumaour, M., Sali, S., Kermadi, S., Zougar, L., Bahfir, A., & Chaieb, Z. (2019). High efficiency silicon solar cells with back ZnTe layer hosting IPV effect: a numerical case study. *Journal of Taibah University for Science*, *13*(1), 696–703. https://doi.org/10.1080/16583655.2019.1623476.

Chen, J., Liu, R., Zhu, L., Chen, W., Dong, C., Wan, Z., Cao, W., Zhang, X., Peng, R., & Wang, M. (2021). Sb_2S_3-based bulk/nano planar heterojunction film solar cells with graphene/polymer composite layer as hole extracting interface. *Materials Letters*, *300*, 130190. https://doi.org/10.1016/j.matlet.2021.130190.

Chen, Z. & Chen, G. (2020). The effect of absorber thickness on the planar Sb_2S_3 thin film solar cell: Trade-off between light absorption and charge separation. *Solar Energy*, *201*, 323–329. https://doi.org/10.1016/j.solener.2020.02.074.

Choi, Y.C., Lee, D.U., Noh, J.H., Kim, E.K., & Seok, S.I. (2014a). Highly improved Sb_2S_3 sensitized-inorganic–organic heterojunction solar cells and quantification of traps by deep-level transient spectroscopy. *Advanced Functional Materials*, *24*(23), 3587–3592. https://doi.org/10.1002/adfm.201304238.

Choi, Y.C., Lee, Y.H., Im, S.H., Noh, J.H., Mandal, T.N., Yang, W.S., & Seok, S.I. (2014b). Efficient inorganic-organic heterojunction solar cells employing $Sb_2(S_x/Se_{1-x})_3$ graded-composition sensitizers. *Advanced Energy Materials*, *4*(7), 1301680. https://doi.org/10.1002/aenm.201301680.

Dixit, K. (2023). *Numerical Simulation and Modeling of thin Film Heterojunction Photovoltaic Cells and its degradation analysis* [Doctoral dissertation]. Dayalbag Educational Institute. https://shodhgangotri.inflibnet.ac.in/handle/20.500.14146/11273.

Eisele, W., Ennaoui, A., Schubert-Bischoff, P., Giersig, M., Pettenkofer, C., Krauser, J., Lux-Steiner, M., Zweigart, S., & Karg, F. (2003). XPS, TEM, and NRA investigations of $Zn(Se,OH)/Zn(OH)_2$ films on $Cu(In,Ga)(S,Se)_2$ substrates for highly efficient solar cells. *Solar Energy Materials and Solar Cells*, *75*(1–2), 17–26. https://doi.org/10.1016/S0927-0248(02)00104-6.

Faheem, M.B., Khan, B., Feng, C., Farooq, M.U., Raziq, F., Xiao, Y., & Li, Y. (2019). All-inorganic perovskite solar cells: energetics, key challenges, and strategies toward commercialization. *ACS Energy Letters*, *5*(1), 290–320. https://doi.org/10.1021/acsenergylett.9b02338.

Green, M.A., Ho-Baillie, A., & Snaith, H.J. (2014). The emergence of perovskite solar cells. *Nature Photonics*, *8*(7), 506–514. https://doi.org/10.1038/NPHOTON.2014.134.

Green, M.A., Emery, K., Hishikawa, Y., Warta, W., & Dunlop, E.D. (2016). Solar cell efficiency tables (version 48). *Progress in Photovoltaics: Research and Applications*, *24*, 905–913. https://doi.org/10.1002/pip.2788.

Gupta, V.K., Sethi, B., Upadhyay, N., Kumar, S., Singh, R., & Singh, L.P. (2011). Iron (III) selective electrode based on S-methyl N-(methylcarbamoyloxy) thioacetamide as a sensing material. *International Journal of Electrochemical Science*, *6*(3), 650–663. http://www.electrochemsci.org/papers/vol6/6030650.pdf.

Jaramillo-Quintero, O.A., Baron-Jaimes, A., Miranda-Gamboa, R.A., & Rincon, M.E. (2021). Cadmium-free ZnS interfacial layer for hydrothermally processed Sb_2S_3 solar cells. *Solar Energy*, *224*, 697–702. https://doi.org/10.1016/j.solener.2021.06.037.

Jin, X., Zhang, L., Jiang, G., Liu, W., & Zhu, C. (2017). High open-circuit voltage of ternary Cu_2GeS_3 thin film solar cells from combustion synthesized Cu-Ge alloy. *Solar Energy Materials and Solar Cells*, *160*, 319–327. https://doi.org/10.1016/j.solmat.2016.11.001.

Koltsov, M., Gopi, S.V., Raadik, T., Krustok, J., Josepson, R., Gržibovskis, R., Vembris, A., & Spalatu, N. (2023). Development of Bi_2S_3 thin film solar cells by close-spaced sublimation and analysis of absorber bulk defects via in-depth photoluminescence analysis. *Solar Energy Materials and Solar Cells*, *254*, 112292. https://doi.org/10.1016/j.solmat.2023.112292.

Kondrotas, R., Chen, C., & Tang, J. (2018). Sb_2S_3 solar cells. *Joule*, *2*(5), 857–878. https://doi.org/10.1016/j.joule.2018.04.003.

Lee, Y.-J., Kim, B.-S., & Ifitiquar, S.M., Park, Ch., Ji, Y. (2014). Silicon solar cells: Past, present and the future. *Journal of the Korean Physical Society*, *65*(3), 355–361. https://doi.org/10.3938/jkps.65.355.

Lee, Y.S., Chua, D., Brandt, R.E., Siah, S.C., Li, J.V., Mailoa, J.P., Lee, S.W., Gordon, R.G., & Buonassisi, T. (2014). Atomic layer deposited gallium oxide buffer layer enables 1.2 V open-circuit voltage in cuprous oxide solar cells. *Advanced Materials*, *26*(27), 4704–4710. https://doi.org/10.1002/adma.201401054.

Lewis, N.S. (2016). Research opportunities to advance solar energy utilization. *Science*, *351*(6271). https://doi.org/10.1126/science.aad1920.

Li, J., Xiong, L., Hu, X., Liang, J., Chen, C., Ye, F., Li, J., Liu, Y., Shao, W., Wang., T., Tao. Ch., & Fang, G. (2022). Manipulating the morphology of CdS/Sb_2S_3 heterojunction using a Mg-doped tin oxide buffer layer for highly efficient solar cells. *Journal of Energy Chemistry*, *66*, 374–381. https://doi.org/10.1016/j.jechem.2021.08.029.

Liu, X., Xiao, X., Yang, Y., Xue, D.-J., Li, D.B., Chen, C., Lu, S., Gao, L., He, Y., Beard, M.C., Wang, G., Chen, S., & Tang, J. (2017). Enhanced Sb_2Se_3 solar cell performance through theory-guided defect control. *Progress in Photovoltaics: Research and Applications*, *25*(10), 861–870. https://doi.org/10.1002/pip.2900.

Louwen, A., van Sark, W., Schropp, R., & Faaij, A. (2016). A cost roadmap for silicon heterojunction solar cells. *Solar Energy Materials and Solar Cells*, *147*, 295–314. https://doi.org/10.1016/j.solmat.2015.12.026.

Ma, G., Wang, C., Zheng, Q., Jin, M., Cheng, S., Lai, Y., Yu, J., & Jia, H. (2020). Ti doped Sb_2S_3 thin film for improved performance of inorganic-organic hybrid solar cells. *Materials Letters*, *260*, 126879. https://doi.org/10.1016/j.matlet.2019.126879.

Michaelson, H.B. (1977). The work function of the elements and its periodicity. *Journal of Applied Physics*, *48*(11), 4729–4733. https://doi.org/10.1063/1.323539.

Moon, S.-J., Itzhaik, Y., Yum, J.-H., Zakeeruddin, S.M., Hodes, G., & Grätzel, M. (2010). Sb_2S_3-based mesoscopic solar cell using an organic hole conductor. *The Journal of Physical Chemistry Letters*, *1*(10), 1524–1527. https://doi.org/10.1021/jz100308q.

Mukherjee, R. (2020). Electrical, thermal, and elastic properties of methylammonium lead bromide single crystal. *Bulletin of Materials Science*, *43*(1), 197. https://doi.org/10.1007/s12034-020-02164-w.

Mukherjee, R., Laves, G., & Nadgorny, B. (2014). Enhancement of high dielectric permittivity in $CaCu_3Ti_4O_{12}$/RuO_2 composites in the vicinity of the percolation threshold. *Applied Physics Letters*, *105*(7). https://doi.org/10.1063/1.4893009.

Nair, P.K., Garcia-Angelmo, A.R., & Nair, M.T.S. (2016). Cubic and orthorhombic SnS thin-film absorbers for tin sulfide solar cells. *Physica Status Solidi (A)*, *213*(1), 170–177. https://doi.org/10.1002/pssa.201532426.

Olopade, M., Adewoyin, A., Chendo, M., & Bolaji, A. (2017). The study of some materials as buffer layer in copper antimony sulphide (CUSbS2) solar cell using SCAPS 1-D. In *IEEE 44th Photovoltaic Specialist Conference (PVSC)* (pp. 2381–2384). https://doi.org/10.1109/PVSC.2017.8366580.

Omrani, M.K., Minbashi, M., Memarian, N., & Kim, D.-H. (2018). Improve the performance of CZTSSe solar cells by applying a SnS BSF layer. *Solid-State Electronics*, *141*, 50–57. https://doi.org/10.1016/j.sse.2017.12.004.

Polman, A., Knight, M., Garnett, E.C., Ehrler, B., & Sinke, W.C. (2016). Photovoltaic materials: Present efficiencies and future challenges. *Science*, *352*(6283). https://doi.org/10.1126/science.aad4424.

Rau, U., Schmidt, M., Jasenek, A., Hanna, G., & Schock, H.W. (2001). Electrical characterization of Cu(In,Ga)Se_2 thin-film solar cells and the role of defects for the device performance. *Solar Energy Materials and Solar Cells*, *67*(4), 37–43. https://doi.org/10.1016/S0927-0248(00)00273-7.

Snaith, H.J. (2018). Present status and future prospects of perovskite photovoltaics. *Nature Materials*, *17*(5), 372–376. https://doi.org/10.1038/s41563-018-0071-z.

Xiao, Y., Wang, H., & Kuang, H. (2020). Numerical simulation and performance optimization of Sb_2S_3 solar cell with a hole transport layer. *Optical Materials*, *108*, 110414. https://doi.org/10.1016/j.optmat.2020.110414.

Xue, D.-J., Liu, S.-Ch., Dai, Ch.M., Chen, S., He, Ch., Zhao, L., Hu, J.-S., & Wan, L.-J. (2017). GeSe thin-film solar cells fabricated by self-regulated rapid thermal sublimation. *Journal of the American Chemical Society*, *139*(2), 958–965. https://doi.org/10.1021/jacs.6b11705.

Zeng, K., Xue, D.-J., & Tang, J. (2016). Antimony selenide thin-film solar cells. *Semiconductor Science and Technology*, *31*(6), 063001. https://doi.org/10.1088/0268-1242/31/6/063001.

Zhang, F., Silver, S.H., Noel, N.K., Ullrich, F., Rand, B.P., & Kahn, A. (2020). Ultraviolet photoemission spectroscopy and Kelvin probe measurements on metal halide perovskites: Advantages and pitfalls. *Advanced Energy Materials*, *10*(26), 1903252. https://doi.org/10.1002/aenm.201903252.

Zhang, W., Eperon, G.E., & Snaith, H.J. (2016). Metal halide perovskites for energy applications. *Nature Energy*, *1*(6), 16048. https://doi.org/10.1038/nenergy.2016.48.

Zhou, H., Chen, Q., Li, G., Luo, S., Song, T.-B., Duan, H.-S., Hong, Z., You, J., Liu, Y., & Yang, Y. (2014). Interface engineering of highly efficient perovskite solar cells. *Science*, *345*(6196), 542–546. https://doi.org/10.1126/science.1254050.